Antimony(III) Fluoride Fluorosulfates: Syntheses and Molecular Structures of Antimony(III) Difluoride Fluorosulfate $[SbF_2(SO_3F)]_x$, Antimony(III) Fluoride Bis(fluorosulfate) $[SbF(SO_3F)_2]_x$, and Antimony(III) Tris(fluorosulfate) $[Sb(SO_3F)_3]_x$

Dingliang Zhang, Steven J. Rettig, James Trotter, and Friedhelm Aubke*

Department of Chemistry, University of British Columbia, Vancouver, BC, Canada V6T 1Z1

Received December 9, 1994[⊗]

Following unsuccessful attempts to confirm the existence of previously reported antimony(I) fluorosulfate, Sb(SO_3F), the reaction of antimony and fluorosulfuric acid is reinvestigated and synthetic routes are developed that allow the preparation of polymeric $[SbF_2(SO_3F)]_x$, $[SbF(SO_3F)_2]_x$, and $[Sb(SO_3F)_3]_x$. Recrystallization from fluorosulfuric acid is found to produce single crystals of all three materials, which are suitable for molecular structure determinations by single-crystal X-ray diffraction. Crystals of $[SbF_2(SO_3F)]_x$ are orthorhombic, a = 13.4035(6) Å, b = 7.1852(6) Å, c = 5.0239(9) Å, Z = 4, and space group $Pna2_1$. Crystals of $[SbF(SO_3F_2)]_x$ are monoclinic, a = 10.7302(8) Å, b = 4.899(1) Å, c = 13.671(1) Å, b = 111.253(7)°, Z = 4, space group $P2_1/c$. Crystals of $[Sb(SO_3F)_3]_x$ are hexagonal, a = 9.5718(9) Å, c = 17.283(1) Å, Z = 6, and space group $P6_5$. Data for all three compounds were collected to high resolution (Mo radiation, $2\theta_{max}$ = 100°) in order to provide accurate structural information. The structures were solved by Patterson ($[SbF_2(SO_3F)]_x$ and $[SbF(SO_3F)_2]_x$) or direct methods ($[Sb(SO_3F)_3]_x$) and were refined by full-matrix least-squares procedures to R = 0.025, 0.028, and 0.030 (R_w = 0.026, 0.027, and 0.027) for 1807, 4572, and 2675 reflections with $I \geq 3\sigma(F^2)$, respectively. The three structures, together with the previously reported structure of $[SbF_3]_x$, allow a detailed comparison for all four members of the series $[SbF_n(SO_3F)_{3-n}]$ for n = 0, 1, 2, or 3. In all structures, fluorines function as asymmetrical, bidentate bridges between two different antimony atoms, while the fluorosulfates are found to form asymmetric O-tridentate bridges. Hence the coordination number for antimony increases from 6 for $[SbF_3]_x$ to 7 for $[SbF_2(SO_3F)]_x$, 8 for $[SbF(SO_3F)_2]_x$, and 9 for $[Sb(SO_3F)_3]_x$. All coordination geometries are highly distorted. According to Sb−O or Sb−F bond distances, the bonds are classified as primary (~2.0 ± 0.1 Å), intermediate (~2.5 ± 0.1 Å), and secondary (~2.9 ± 0.1 Å). The primary coordination geometries are trigonal pyramidal for SbF_3, $[SbF(SO_3F)_2]_x$, and $[Sb(SO_3F)_3]_x$ and distorted square pyramidal for $[SbF_2(SO_3F)]_x$.

Introduction

While the oxidation states +3 and +5 are commonly found for antimony in inorganic and organic compounds,[1] there are a limited number of reported species where the formal oxidation state of antimony appears to be lower than +3. The known examples include several gaseous, monomeric molecules of the type SbO or SbX, X = H, F, Cl, Br, or I, or SbH_2, which are usually generated by flash photolysis of SbH_3 or the corresponding trihalides and are studied by kinetic spectroscopy.[1] In these species antimony is uni- or divalent. There appears to be little doubt regarding the transient existence of these molecular fragments in the gas phase.

In the condensed phase the situation is much less clear. A number of claims have been made, all in short, preliminary publications. They date back at least 20 years and point to the possible existence of low-valent antimony species. The polyatomic cations Sb_8^{2+} and Sb_4^{2+} are claimed to exist in strong protonic acids or in solid compounds like $Sb_4(SO_3F)_2$.[2,3] These reports have been subsequently discredited[4] when the reported UV−visible spectra could be attributed to the polyatomic sulfur cations S_8^{2+} and S_4^{2+}, seemingly formed in the reduction of HSO_3F or H_2SO_4 by antimony.[4] In the same communication, the formation and isolation of a colorless, univalent antimony salt of the composition Sb(SO_3F) is claimed,[4] but neither spectroscopic nor analytical details on this intriguing material appear to have been reported in the open literature. It had previously been reported that antimony will dissolve in boiling HSO_3F (~163 °C) to give a colorless solution,[5] but the nature of the dissolution process had not been elucidated at that time.

The oxidation state +1 for antimony is also suggested for $Sb[AsF_6]$, formed by oxidation of antimony with AsF_5 in liquid SO_2.[6] Evidence rests on the identification of $[AsF_6]^-$ by ^{19}F NMR and IR spectroscopy, while a magnetic susceptibility measurement at 18 °C is interpreted in terms of very weak temperature-dependent paramagnetism due to a cluster cation of the type $[Sb_n]^{n+}$.[6]

We have been interested for some time in antimony(V) fluorosulfate derivatives[7] and have studied recently the oxidation of elemental antimony by bis(fluorosulfuryl) peroxide, $S_2O_6F_2$, by analogy to earlier work on the oxidation of niobium and tantalum.[8] The formation of a white, fluorosulfate-containing solid in the initial stages of the oxidation reaction motivated us to reinvestigate the reported formation of Sb(SO_3F)[4] in the reaction of antimony with HSO_3F.

The results of this reinvestigation are discussed in this report and may be summarized as follows:

* Author to whom correspondence should be addressed.

[⊗] Abstract published in *Advance ACS Abstracts,* May 1, 1995.

(1) Moss, K. C.; Smith, M. A. R. *Int. Rev. Science Inorg. Chem.* **1975**, *Series II*, *2*, 221 and references therein.
(2) Paul, R. C.; Paul, K. K.; Malhotra, K. C. *J. Chem. Soc., Chem. Commun.* **1970**, 453.
(3) Malhotra, K. C.; Puri, J. K. *Inorg. Nucl. Chem. Lett.* **1971** (7), 209.
(4) Gillespie, R. J.; Vaidya, O. C. *J. Chem. Soc., Chem. Commun.* **1972**, 40.
(5) Brazier, J. N.; Woolf, A. A. *J. Chem. Soc. A* **1967**, 99.
(6) Dean, P. A. W.; Gillespie, R. J. *J. Chem. Soc., Chem. Commun.* **1970**, 853.
(7) Wilson, W. W.; Aubke, F. *J. Fluorine Chem.* **1979**, *13*, 431.
(8) (a) Cicha, W. V.; Aubke, F. *J. Am. Chem. Soc.* **1989**, *111*, 4328. (b) Zhang, D.; Aubke, F. *J. Fluorine Chem.* **1992**, *58*, 81.

0020-1669/95/1334-3153$09.00/0

(i) We have been unable to obtain pure antimony(I) fluorosulfate in spite of numerous attempts. Furthermore, we find no evidence for the presence of univalent antimony in the white materials produced in the reaction of antimony with HSO_3F.

(ii) All white solid materials obtained by the use of various synthetic approaches are found to contain only antimony in the +3 oxidation state. By recrystallization of the white solids from fluorosulfuric acid we have obtained single crystals of the previously unknown polymeric antimony(III) fluoro fluorosulfates $[SbF_2(SO_3F)]_x$ and $[SbF(SO_3F)_2]_x$ and of the previously reported $[Sb(SO_3F)_3]_x$[4] and report here the molecular structures of all three compounds.

(iii) Including the known molecular structure of antimony(III) fluoride, SbF_3,[9] we can now undertake a structural comparison for all four members in the series $[Sb^{III}F_n(SO_3F)_{3-n}]_x$, $n = 0-3$, which are all polymers that feature asymmetric bidentate, fluoro- and O-tridentate fluorosulfato bridges, involved in primary- intermediate-, and secondary-bond formation.

Experimental Section

Chemicals. Antimony metal powder, 99.5% pure, 100 mesh, was obtained from Matheson Coleman & Bell. Antimony trifluoride (SbF_3, 99.9% pure), antimony(III) ethoxide ($Sb(OC_2H_5)_3$, $n_{d,20} = 1.495$) and α-naphthoflavone (7,8-benzoflavone, 97% pure) were obtained from Aldrich. The reagents KBr and $KBrO_3$ of A.R. grade were obtained from Fisher Scientific Co. and Mallinckrodt Chemicals, respectively. Technical-grade fluorosulfuric acid, HSO_3F, was obtained from Orange County Chemicals, Santa Anna, CA, and purified by double distillation in a counter flow of dry N_2 under atmospheric pressure, as described previously.[10] Bis(fluorosulfuryl) peroxide is prepared by catalytic (AgF_2) fluorination of SO_3 as described previously.[11]

Analysis. Microanalysis for C, H, and S was performed by Mr. P. Borda of this Department. Antimony content of the samples was analyzed by us employing a potassium bromate titration with α-naphthoflavone as indicator.[12,13]

Instrumentation. Infrared spectra were obtained on a Bomen MB-102 FT-IR spectrometer, and FT-Raman spectra were obtained on a Bruker FRA 106 Raman module mounted on a TFS66V FT-IR optical bench. To handle hygroscopic material, a "DRI-LAB" Model DL-001-S-G drybox (Vacuum Atmosphere Corp., Hawthorne, CA) filled with dry N_2 was used.

Synthesis of $[SbF_2(SO_3F)]_x$. (a) Reaction of Antimony with HSO_3F. The compound was obtained in the reaction of antimony and HSO_3F. In a typical preparation, 0.5428 g (4.46 mmol) of antimony powder and 6.7796 g (67.7 mmol) of HSO_3F were added into a one-body reactor fitted with a Kontes Teflon-stem stopcock. The reaction proceeded smoothly at room temperature. Sulfur dioxide was detected by infrared spectroscopy as a reaction product in the gas phase above the reaction mixture. As the reaction proceeded, formation of a yellow solid was also observed. The mixture was stirred for about 2 days until all metal powder was consumed and a mixture of yellow and white solid material had formed. After removal of the yellow solid S_8 by hot filtration *in vacuo* at 50 °C, 0.7064 g of white powder was obtained from the filtrate after cooling and filtration, followed by drying the product *in vacuo*. The isolated yield was 61%. The white powder did not melt or decompose below 250 °C. Anal. Calcd for $SbSF_3O_3$: Sb, 47.04. Found: Sb, 47.5.

(b) Solvolysis of $SbF_2(OEt)$ in an Excess of HSO_3F. The precursor $SbF_2(OC_2H_5)$ was first prepared by a stoichiometric redistribution reaction of SbF_3 and $Sb(OC_2H_5)_3$ (2:1 mole ratio) in acetonitrile as reported previously.[14] In a typical preparation 2.010 g (10.34 mmol) of SbF_3 and 1.393 g (5.42 mmol) of $Sb(OC_2H_5)_3$ were combined in a 50-mL two-part reactor in a drybox. About 25 mL of previously dried CH_3CN was added to the reactor by vacuum transfer. The mixture was then stirred for 1 day at room temperature. A fine white powder was obtained after filtration. The powder was dried *in vacuo* at room temperature for 1 day to remove the solvent CH_3CN completely. A 2.01 g amount of white powder was obtained (isolated yield 84%). Anal. Calcd for $C_2H_5F_2OSb$: Sb, 59.5. Found: Sb, 60.4.

$[SbF_2(SO_3F)]_x$ was obtained by subsequent solvolysis of $SbF_2(OC_2H_5)$ in HSO_3F. In a typical preparation 0.5 g of $SbF_2(OC_2H_5)$ was added to a 50-mL reactor inside the drybox. Then ~5 mL of HSO_3F was transferred into the reactor *in vacuo*. The mixture was stirred first at room temperature overnight and then at 50 °C until all the solid had dissolved to form a colorless solution. Removal of all volatiles *in vacuo* produced $[SbF_2(SO_3F)]_x$.

To prepare crystals suitable for single-crystal X-ray diffraction analysis, the HSO_3F solution was allowed to cool very slowly to room temperature. Colorless crystals were obtained.

Synthesis of $[SbF(SO_3F)_2]_x$. A 0.1515 g (1.244 mmol) amount of antimony metal was added to a reaction ampule fitted with a Kontes Teflon-stem stopcock. Then 11.2 g (56.50 mmol) of $S_2O_6F_2$ was transferred into the reactor *in vacuo*. The reaction was allowed to proceed slowly at room temperature for 2 weeks. After removal of all volatiles (pumping for 48 h), 0.497 g of a gray sticky mass was obtained. (This gray sticky material appears to be a mixture of a white solid, a black metal powder, and a colorless, viscous liquid.) Excess HSO_3F was then added *in vacuo* to the residue. After 1 day all black metal powder had disappeared and solid yellow granules were observable, together with a white powder. When the mixture was heated to 50 °C, the white solid dissolved in HSO_3F, but the yellow material, presumed to be S_8, remained in suspension. The yellow solid was then removed by filtration *in vacuo* at 50 °C, using an apparatus similar to the one described by Shriver.[15] A white precipitate appeared as the filtrate cooled down to room temperature.

To prepare a crystal suitable for single-crystal X-ray diffraction analysis, the filtrate was warmed up again to 50 °C *in vacuo* to dissolve the white solid, resulting in a colorless solution. The solution was then allowed to cool down very slowly to room temperature. Colorless needlelike crystals were obtained, and fragments were used for the structure determination and to record an IR spectrum. Bands in cm^{-1}: 1348 vs; 1201 m, sh; 1150 vs, br; 1030 vs; 927 ms, sh; 867 vw; 849 w, 815 s; 710 sh, br; 617 m; 605 m; 586 s; 574 s; 556 ms; 453 m; 422 ms, 408 w.

Synthesis of $[Sb(SO_3F)_3]_x$. Antimony tris(fluorosulfate) was synthesized by controlled oxidation of antimony with $S_2O_6F_2$ in HSO_3F. In a typical preparation, 0.4911 g (4.034 mmol) of antimony powder and 15.51 g (155 mmol) of HSO_3F were added into a two-part reactor inside the drybox. To suppress the reaction between antimony and HSO_3F the reactor was taken out of the drybox and cooled to liquid-nitrogen temperature immediately after the HSO_3F was added. $S_2O_6F_2$ was transferred *in vacuo* from a preweighed vessel. The weight of the container was tracked during the transfer. In this manner slightly more than the stoichiometric amount of $S_2O_6F_2$ (1.5667 g, 7.913 mmol) was added to give a Sb to $S_2O_6F_2$ mole ratio of 1:1.96. The reaction proceeded smoothly at room temperature. The mixture was stirred for about 2 days until all the metal powder was consumed and a white solid resulted. A hot filtration was performed *in vacuo* at 50 °C to ensure that all yellow solid was separated from the white precipitate. After the hot filtration, the filtrate solution was cooled to room temperature to allow the product to precipitate again. A 0.93 g (2.22 mmol) amount of white powder was collected by filtration *in vacuo*, which corresponds to an isolated yield of 55%. Anal. Calcd for $SbS_3O_9F_3$: Sb, 29.06. Found: Sb, 28.7. $[Sb(SO_3F)_3]_x$ melted with decomposition at 153 °C. Vibrational spectral data are as follows: IR $\bar{\nu}$ (cm^{-1}): 1389 s, 1341 vs, 1235 ms, sh, 1209 vs, 1188 vs, 1074 ms, 1046 ms, 990 s, 841 s, 825 ms, sh, 625 w, 607 s, 570 s, 558 m, sh, 550 s, 444 mw, 429 ms, 407 w. Raman $\Delta\bar{\nu}$ (cm^{-1}): 1395 w, 1386 vw, 1365 m, 1339 mw, b, 1232 m, 1208 s, 1188 m, 1074 m, sh, 1063 m, 1043 w, 871 vs, 839 w, 827 w, 627 ms, 611 m, 584 m, 565 mw, 555 w, 549 w, 444 m, 431 ms, 410 m, 398 w, 248 s 213 mw, 169 vw, 147

(9) Edwards, A. J. *J. Chem. Soc. A* **1970**, 2751.
(10) Barr, J.; Gillespie, R. J.; Thompson, R. C. *Inorg. Chem.* **1964**, *3*, 1149.
(11) Cady, G. H.; Shreeve, J. M. *Inorg. Synth.* **1963**, *7*, 124.
(12) Skoog, D. A.; West, D. M. *Fundamentals of Analytical Chemistry*, 3rd ed.; Holt, Rinehart, & Winston: New York, 1976; p 35.
(13) Morries, P. In *Comprehensive Analytical Chemistry*; Wilson, C. L., Wilson, D. W., Eds.; Elsevier: New York, 1962; Vol. 1c, p 252.
(14) Hass, D.; Cech, D. Z. *Chem.* **1970**, *10*, 33.
(15) Shriver, D. F. *The Manipulation of Air-Sensitive Compounds*; McGraw-Hill: New York, 1969.

Table 1. Crystallographic Data[a]

compd	$[SbF_2(SO_3F)]_x$	$[SbF(SO_3F)_2]_x$	$[Sb(SO_3F)_3]_x$
formula	F_3O_3SSb	$F_3O_6S_2Sb$	$F_3O_9S_3Sb$
fw	258.80	338.86	418.92
cryst system	orthorhombic	monoclinic	hexagonal
space group	$Pna2_1$	$P2_1/c$	$P6_5$
a, Å	13.4035(6)	10.7302(8)	9.5718(9)
b, Å	7.1852(6)	4.899(1)	9.5718(9)
c, Å	5.0239(9)	13.671(1)	17.283(1)
β, deg	90	111.253(7)	90
V, Å^3	483.8(1)	669.7(3)	1371.3(3)
Z	4	4	6
ϱ_{calc}, g/cm^3	3.553	3.361	3.043
T, °C	21	21	21
λ, Å	0.710 69	0.710 69	0.710 69
μ, cm^{-1}	61.40	47.96	37.85
transm factors (relative)	0.84−1.00	0.54−1.00	0.81−1.00
$R(F)$	0.025	0.028	0.030
$R_w(F)$	0.026	0.027	0.027

[a] $R = \sum||F_o| - |F_c||/\sum|F_o|$; $R_w = (\sum w(|F_o| - |F_c|)^2/\sum w|F_o|^2)^{1/2}$.

w, 130 vw, 99 w. To obtain crystals for X-ray analysis, the hot filtrate solution was allowed slowly to cool to room temperature. The crystals were separated by filtration and mounted in the inert-atmosphere box into capillaries.

X-ray Crystallographic Analyses of $[SbF_2(SO_3F)]_x$, $[SbF(SO_3F)_2]_x$, and $[Sb(SO_3F)_3]_x$. Crystallographic data are given in Table 1. The final unit-cell parameters were obtained by least-squares on the setting angles for 25 reflections with $2\theta = 57.1$-$59.8°$ for $[SbF_2(SO_3F]_x$, 68.5−69.7° for $[SbF(SO_3F)_2]_x$, and 50.7-59.1° for $[Sb(SO_3F)_3]_x$. The intensities of three standard reflections, measured every 200 reflections throughout the data collection, showed only small random variations for $[SbF(SO_3F)_2]_x$ and $[Sb(SO_3F)_3]_x$ and decayed uniformly by 10.4% for $[SbF_2(SO_3F)]_x$. The data were processed[16] and corrected for Lorentz and polarization effects, decay (for $[SbF_2(SO_3F)]_x$), and absorption (empirical, based on azimuthal scans for three reflections).

The structures of $[SbF_2(SO_3F)]_x$ and $[SbF(SO_3F)_2]_x$ were solved by conventional heavy-atom methods, the coordinates of the Sb atom being determined from the Patterson function and those of the remaining atoms from subsequent difference Fourier syntheses. The structure of $[Sb(SO_3F)_3]_x$ was solved by direct methods. The structure analysis of $[SbF_2(SO_3F)]_x$ was initiated in the noncentrosymmetric space group $Pna2_1$ on the basis of the E-statistics and the appearance of the Patterson function. This choice was confirmed by subsequent calculations. All atoms were refined with anisotropic thermal parameters. Corrections for secondary extinction were applied for two of the structures (Zachariasen isotropic type I), the final values of the extinction coefficient being $2.93(3) \times 10^{-5}$ for $[SbF_2(SO_3F)]_x$ and $2.96(11) \times 10^{-7}$ for $[SbF(SO_3F)_2]_x$. A parallel refinement of the mirror-image structure of $[SbF_2(SO_3F)]_x$ (opposite polarity) gave higher residuals, the R and R_w factor ratios being 1.023 and 1.022, respectively. Refinement of the mirror-image structure of $[Sb(SO_3F)_3]_x$ in the enantiomorphic space group $P6_1$ also gave significantly higher residuals, the R and R_w factor ratios being 1.052 and 1.063, respectively. Neutral atom scattering factors[17a] and anomalous dispersion corrections[17b] were taken from *The International Tables for X-Ray Crystallography*.

Final atomic coordinates and equivalent isotropic thermal parameters and bond distances and angles are listed in Tables 2 and 3 for $[Sb(SO_3F)_3]_x$, in Tables 4 and 5 for $[SbF(SO_3F)_2]_x$, and in Tables 6 and 7 for $[SbF_2(SO_3F)]_x$. Complete tables of crystallographic data, anisotropic thermal parameters, torsion angles, and nonbonded contacts for the three structures are included as supplementary material. Structure factors are available from the authors upon request.

Results and Discussion

Synthesis. Initial attempts aimed at the synthesis of $Sb(SO_3F)$ have involved the reaction of antimony and fluorosulfuric acid.

Table 2. Fractional Atomic Coordinates and B_{eq} Values (Å^2) for $[SbF_2(SO_3F)]_x$ (Esd's in Parentheses)

atom	x	y	z	B_{eq}[a]
Sb(1)	0.710898(11)	0.21402(2)	0.8137	1.484(5)
S(1)	0.45037(5)	0.22561(11)	0.6064(2)	1.73(2)
F(1)	0.4461(3)	0.3085(4)	0.3264(12)	5.6(2)
F(2)	0.6973(2)	0.0281(4)	0.5485(6)	2.9(1)
F(3)	0.7240(2)	0.3954(4)	0.5335(6)	2.8(1)
O(1)	0.4350(2)	0.0332(4)	0.5735(7)	2.4(1)
O(2)	0.5449(2)	0.2854(4)	0.7102(11)	3.5(1)
O(3)	0.3716(2)	0.3274(5)	0.7413(8)	3.5(1)

[a] $B_{eq} = (8/3)\pi^2\sum\sum U_{ij}a_i^*a_j^*(\mathbf{a}_i\cdot\mathbf{a}_j)$.

Table 3. Bond Lengths (Å) and Angles (deg) for $[SbF_2(SO_3F)]_x$ (Esd's in parentheses)[a]

Sb(1)−F(2)	1.896(3)	Sb(1)−F(2)[a]	2.828(3)
Sb(1)−F(3)	1.927(3)	Sb(1)−F(3)[b]	2.687(2)
Sb(1)−O(1)[c]	2.946(3)	Sb(1)−O(2)	2.342(3)
Sb(1)−O(3)[d]	2.204(3)	S(1)−F(1)	1.529(6)
S(1)−O(1)	1.408(3)	S(1)−O(2)	1.435(3)
S(1)−O(3)	1.453(3)		
F(2)−Sb(1)−F(2)[a]	153.8(1)	F(2)−Sb(1)−F(3)	88.4(2)
F(2)−Sb(1)−F(3)[b]	73.7(1)	F(2)−Sb(1)−O(1)[c]	79.8(1)
F(2)−Sb(1)−O(2)	84.7(1)	F(2)−Sb(1)−O(3)[d]	83.3(1)
F(2)[a]−Sb(1)−F(3)	74.1(1)	F(2)[a]−Sb(1)−F(3)[b]	111.54(10)
F(2)[a]−Sb(1)−O(1)[c]	125.80(9)	F(2)[a]−Sb(1)−O(2)	109.35(9)
F(2)[a]−Sb(1)−O(3)	75.6(1)	F(3)−Sb(1)−F(3)[b]	147.9(1)
F(3)−Sb(1)−O(1)[c]	142.38(8)	F(3)−Sb(1)−O(2)	77.1(1)
F(3)−Sb(1)−O(3)[d]	83.2(1)	F(3)[b]−Sb(1)−O(2)	125.89(9)
F(3)[b]−Sb(1)−O(1)[c]	61.31(7)	F(3)[b]−Sb(1)−O(3)[d]	68.62(9)
O(2)−Sb(1)−O(1)[c]	66.4(1)	O(2)−Sb(1)−O(3)[d]	157.1(2)
O(3)−Sb(1)−O(1)[c]	129.79(9)	F(1)−S(1)−O(1)	105.6(2)
F(1)−S(1)−O(2)	104.5(3)	F(1)−S(1)−O(3)	101.9(2)
O(1)−S(1)−O(2)	117.8(1)	O(1)−S(1)−O(3)	116.3(2)
O(2)−S(1)−O(3)	108.7(2)	Sb(1)−F(2)−Sb(1)[e]	144.5(1)
Sb(1)−F(3)−Sb(1)[f]	155.0(1)	Sb(1)[g]−O(1)−S(1)	137.8(2)
Sb(1)−O(2)−S(1)	148.6(2)	Sb(1)[h]−O(3)−S(1)	136.0(2)

[a] Superscripts refer to the symmetry operations: (a) $^3/_2 - x$, $^1/_2 + y$, $^1/_2 + z$; (b) $^3/_2 - x$, $-^1/_2 + y$, $^1/_2 + z$; (c) $1 - x$, $-y$, $^1/_2 + z$; (d) $^1/_2 + x$, $^1/_2 - y$, z; (e) $^3/_2 - x$, $-^1/_2 + y$, $-^1/_2 + z$; (f) $^3/_2 - x$, $^1/_2 + y$, $-^1/_2 + z$; (g) $1 - x$, $-y$, $-^1/_2 + z$; (h) $-^1/_2 + x$, $^1/_2 - y$, z.

Table 4. Fractional Atomic Coordinates and B_{eq} Values (Å^2) for $[SbF(SO_3F)_2]_x$ (Esd's in Parentheses)

atom	x	y	z	B_{eq}[a]
Sb(1)	0.248637(11)	0.13796(3)	0.241477(9)	1.470(3)
S(1)	0.57252(4)	0.24031(10)	0.38861(3)	1.38(1)
S(2)	0.08697(4)	0.33616(11)	0.40414(3)	1.48(1)
F(1)	0.25221(12)	−0.2368(3)	0.27610(11)	2.07(4)
F(2)	0.61238(13)	0.3524(3)	0.50090(10)	2.66(5)
F(3)	−0.00097(14)	0.0883(3)	0.40533(12)	2.86(5)
O(1)	0.43215(14)	0.1646(4)	0.36963(12)	2.32(5)
O(2)	0.57961(15)	0.4693(4)	0.32515(12)	2.19(5)
O(3)	0.6589(2)	0.0191(4)	0.39564(14)	2.75(6)
O(4)	0.19217(14)	0.2111(4)	0.37341(12)	2.24(5)
O(5)	0.00027(14)	0.5118(4)	0.32445(11)	2.09(5)
O(6)	0.13756(14)	0.4364(4)	0.50816(11)	2.33(5)

[a] $B_{eq} = (8/3)\pi^2\sum\sum U_{ij}a_i^*a_j^*(\mathbf{a}_i\cdot\mathbf{a}_j)$.

Our observations confirm the conclusions by Gillespie and Vaidya[4] that dissolution of Sb at 25 °C in doubly distilled HSO_3F[10] is indeed an oxidation of antimony, which leads, depending on the reactant ratio, either to a colorless solution or a white precipitate, as claimed earlier.[4,5] However, in addition to SO_2 as reduced byproduct, identified here by its IR spectrum in the gas phase, a yellow, solid material is formed, which is subsequently found to be elemental sulfur, S_8. Addition of $S_2O_6F_2$ to the reaction mixture at this point produces blue-green solutions, with the color due to the polysulfur cations.[4,18]

(16) *teXsan*: *Crystal Structure Analysis Package*; Molecular Structure Corp.: The Woodlands, TX, 1985 and 1992.
(17) (a) *International Tables for X-Ray Crystallography*; Kynoch Press: Birmingham, U.K., 1974; Vol. IV, pp 99−102. (b) *International Tables for Crystallography*; Kluwer Academic Publishers: Boston, MA, 1992; Vol. C, pp 200−206.
(18) Gillespie, R. J.; Passmore, J. *Adv. Inorg. Chem. Radiochem.* **1975**, *17*, 49.

Table 5. Bond Lengths (Å) and Angles (deg) for $[SbF(SO_3F)_2]_x$ (Esd's in Parentheses)[a]

Sb(1)−F(1)	1.893(1)	Sb(1)−O(1)	2.113(1)
Sb(1)−O(2)[a]	2.475(2)	Sb(1)−O(4)	2.131(1)
Sb(1)−O(5)[b]	2.566(1)	Sb(1)−O(6)[c]	2.995(2)
Sb(1)−O(3)[d]	3.055(2)	Sb(1)−F(1)[e]	3.098(2)
S(1)−F(2)	1.538(1)	S(1)−O(1)	1.480(1)
S(1)−O(2)	1.437(2)	S(1)−O(3)	1.407(2)
S(2)−F(3)	1.542(2)	S(2)−O(4)	1.473(1)
S(2)−O(5)	1.435(2)	S(2)−O(6)	1.414(2)
F(1)−Sb(1)−O(1)	85.66(6)	F(1)−Sb(1)−O(2)[a]	79.52(6)
F(1)−Sb(1)−O(4)	86.43(7)	F(1)−Sb(1)−O(5)[b]	77.20(5)
F(1)−Sb(1)−O(6)[c]	96.47(5)	F(1)−Sb(1)−O(3)[d]	139.87(5)
F(1)−Sb(1)−F(1)[e]	157.35(7)	O(1)−Sb(1)−O(2)[a]	74.41(5)
O(1)−Sb(1)−O(4)	75.71(6)	O(1)−Sb(1)−O(5)[b]	147.66(5)
O(1)−Sb(1)−O(6)[c]	141.46(5)	O(1)−Sb(1)−O(3)[d]	93.36(5)
O(1)−Sb(1)−F(1)[e]	81.72(6)	O(2)[a]−Sb(1)−O(4)	147.75(5)
O(2)[a]−Sb(1)−O(5)[b]	127.56(5)	O(2)[a]−Sb(1)−O(6)[c]	68.25(5)
O(2)[a]−Sb(1)−O(3)[d]	61.80(6)	O(2)[a]−Sb(1)−F(1)[e]	114.63(5)
O(4)−Sb(1)−O(5)[b]	76.04(5)	O(4)−Sb(1)−O(6)[c]	142.78(5)
O(4)−Sb(1)−O(3)[d]	132.21(6)	O(4)−Sb(1)−F(1)[e]	72.30(6)
O(5)[b]−Sb(1)−O(6)[c]	68.58(4)	O(5)[b]−Sb(1)−O(3)[d]	117.38(5)
O(5)[b]−Sb(1)−F(1)[e]	104.21(4)	O(6)[c]−Sb(1)−O(3)[d]	60.87(5)
O(6)[c]−Sb(1)−F(1)[e]	105.13(5)	O(3)[d]−Sb(1)−F(1)[e]	60.04(4)
F(2)−S(1)−O(1)	99.30(8)	F(2)−S(1)−O(2)	105.5(1)
F(2)−S(1)−O(3)	105.6(1)	O(1)−S(1)−O(2)	111.3(1)
O(1)−S(1)−O(3)	115.0(1)	O(2)−S(1)−O(3)	117.7(1)
F(3)−S(2)−O(4)	102.2(1)	F(3)−S(2)−O(5)	104.45(9)
F(3)−S(2)−O(6)	106.0(1)	O(4)−S(2)−O(5)	112.7(1)
O(4)−S(2)−O(6)	112.13(9)	O(5)−S(2)−O(6)	117.5(1)
Sb(1)−F(1)−Sb(1)[f]	157.35(7)	Sb(1)−O(1)−S(1)	138.1(1)
Sb(1)[d]−O(2)−S(1)	133.8(1)	Sb(1)[a]−O(3)−S(1)	141.4(1)
Sb(1)−O(4)−S(2)	142.5(1)	Sb(1)[g]−O(5)−S(2)	135.8(1)
Sb(1)[h]−O(6)−S(2)	152.7(1)		

[a] Superscripts refer to the symmetry operations: (a) $1 - x, -1/2 + y, 1/2 - z$; (b) $-x, -1/2 + y, 1/2 - z$; (c) $x, 1/2 - y, -1/2 + z$; (d) $1 - x, 1/2 + y, 1/2 - z$; (e) $x, 1 + y, z$; (f) $x, -1 + y, z$; (g) $-x, 1/2 + y, 1/2 - z$; (h) $x, 1/2 - y, 1/2 + z$.

Table 6. Fractional Atomic Coordinates and B_{eq} Values (Å^2) for $[Sb(SO_3F)_3]_x$ (Esd's in Parentheses)

atom	*x*	*y*	*z*	B_{eq}[a]
Sb(1)	0.61969(3)	0.36227(3)	0.3712	1.642(6)
S(1)	0.40119(10)	0.31440(10)	0.21052(6)	1.55(2)
S(2)	0.61249(11)	0.71711(10)	0.36512(7)	1.62(2)
S(3)	0.40734(12)	0.31527(13)	0.53117(7)	2.09(3)
F(1)	0.2404(3)	0.1542(4)	0.2107(2)	4.3(1)
F(2)	0.7872(3)	0.8491(4)	0.3484(2)	3.6(1)
F(3)	0.2248(4)	0.1993(5)	0.5346(3)	4.6(1)
O(1)	0.4361(3)	0.3405(4)	0.2942(2)	1.82(8)
O(2)	0.3639(4)	0.4278(5)	0.1777(2)	2.6(1)
O(3)	0.5117(4)	0.2853(4)	0.1690(2)	2.3(1)
O(4)	0.6365(4)	0.5866(4)	0.3952(2)	2.2(1)
O(5)	0.5323(4)	0.6837(4)	0.2932(2)	2.7(1)
O(6)	0.5613(4)	0.7828(4)	0.4251(2)	2.4(1)
O(7)	0.4350(3)	0.2805(3)	0.4500(2)	2.04(8)
O(8)	0.4768(5)	0.2580(4)	0.5860(2)	3.2(1)
O(9)	0.4309(5)	0.4716(4)	0.5404(2)	3.2(1)

[a] $B_{eq} = (8/3)\pi^2\sum\sum U_{ij}a_i^*a_j^*(\mathbf{a}_i\cdot\mathbf{a}_j)$.

The solid product mixture is conveniently separated by addition of further fluorosulfuric acid. Heating to 50 °C results in dissolution of the white precipitate only. Filtration of the hot solution leaves S_8 as a residue. From the colorless filtrate, a white, crystalline material forms on cooling to room temperature. Isolation of this material is accomplished either by filtration at room temperature or by the removal of all volatiles *in vacuo*. The advantage of this separation procedure is the formation of single crystals on slow cooling of the filtrate solution.

Initial attempts to characterize the white crystalline material result in the conclusions that antimony is in the +3 oxidation state and that the material has the approximate composition $SbF_n(SO_3F)_{3-n}$ with $n = 1.6-1.8$. Variations in composition for different preparations suggest a product mixture with the fluoride fluorosulfates of antimony(III), $[SbF_2(SO_3F)]_x$, $[SbF(SO_3F)_2]_x$, $[Sb(SO_3F)_3]_x$, and possibly $[SbF_3]_x$ as components of this mixture.

Table 7. Bond Lengths (Å) and Angles (deg) for $[Sb(SO_3F)_3]_x$ (Esd's in Parentheses)[a]

Sb(1)−O(1)	2.129(3)	Sb(1)−O(2)[a]	2.550(3)
Sb(1)−O(3)[b]	2.642(3)	Sb(1)−O(4)	2.112(3)
Sb(1)−O(5)[a]	2.834(3)	Sb(1)−O(6)[c]	2.615(3)
Sb(1)−O(7)	2.052(3)	Sb(1)−O(8)[d]	3.009(4)
Sb(1)−O(9)[c]	2.977(3)	S(1)−F(1)	1.536(3)
S(1)−O(1)	1.477(3)	S(1)−O(2)	1.419(3)
S(1)−O(3)	1.417(3)	S(2)−F(2)	1.537(3)
S(2)−O(4)	1.474(3)	S(2)−O(5)	1.412(3)
S(2)−O(6)	1.421(3)	S(3)−F(3)	1.533(3)
S(3)−O(7)	1.496(3)	S(3)−O(8)	1.417(3)
S(3)−O(9)	1.407(3)		
O(1)−Sb(1)−O(2)[a]	71.3(1)	O(1)−Sb(1)−O(3)[b]	145.6(1)
O(1)−Sb(1)−O(4)	82.1(1)	O(1)−Sb(1)−O(5)[a]	136.9(1)
O(1)−Sb(1)−O(6)[c]	75.9(1)	O(1)−Sb(1)−O(7)	82.3(1)
O(1)−Sb(1)−O(8)[d]	91.2(1)	O(1)−Sb(1)−O(9)[c]	142.0(1)
O(2)[a]−Sb(1)−O(3)[b]	126.3(1)	O(2)[a]−Sb(1)−O(4)	145.1(1)
O(2)[a]−Sb(1)−O(5)[a]	65.9(1)	O(2)[a]−Sb(1)−O(6)[c]	120.77(10)
O(2)[a]−Sb(1)−O(7)	72.1(1)	O(2)[a]−Sb(1)−O(8)[d]	65.9(1)
O(2)[a]−Sb(1)−O(9)[c]	110.2(1)	O(3)[b]−Sb(1)−O(4)	68.0(1)
O(3)[b]−Sb(1)−O(5)[a]	65.90(10)	O(3)[b]−Sb(1)−O(6)[c]	108.6(1)
O(3)[b]−Sb(1)−O(7)	77.4(1)	O(3)[b]−Sb(1)−O(8)[d]	122.46(9)
O(3)[b]−Sb(1)−O(9)[c]	65.71(10)	O(4)−Sb(1)−O(5)[a]	133.1(1)
O(4)−Sb(1)−O(6)[c]	71.7(1)	O(4)−Sb(1)−O(7)	82.5(1)
O(4)−Sb(1)−O(8)[d]	138.4(1)	O(4)−Sb(1)−O(9)[c]	104.7(1)
O(5)[a]−Sb(1)−O(6)[c]	131.88(9)	O(5)[a]−Sb(1)−O(7)	79.7(1)
O(5)[a]−Sb(1)−O(8)[d]	76.8(1)	O(5)[a]−Sb(1)−O(9)[c]	63.1(1)
O(6)[c]−Sb(1)−O(7)	148.1(1)	O(6)[c]−Sb(1)−O(8)[d]	66.94(10)
O(6)[c]−Sb(1)−O(9)[c]	71.2(1)	O(7)−Sb(1)−O(8)[d]	137.3(1)
O(7)−Sb(1)−O(9)[c]	135.3(1)	O(8)[d]−Sb(1)−O(9)[c]	58.67(10)
F(1)−S(1)−O(1)	101.3(2)	F(1)−S(1)−O(2)	104.8(2)
F(1)−S(1)−O(3)	106.2(2)	O(1)−S(1)−O(2)	112.6(2)
O(1)−S(1)−O(3)	113.7(2)	O(2)−S(1)−O(3)	116.5(2)
F(2)−S(2)−O(4)	101.3(2)	F(2)−S(2)−O(5)	105.4(2)
F(2)−S(2)−O(6)	104.3(2)	O(4)−S(2)−O(5)	114.6(2)
O(4)−S(2)−O(6)	110.6(2)	O(5)−S(2)−O(6)	118.3(2)
F(3)−S(3)−O(7)	98.1(2)	F(3)−S(3)−O(8)	106.2(2)
F(3)−S(3)−O(9)	106.5(2)	O(7)−S(3)−O(8)	111.8(2)
O(7)−S(3)−O(9)	113.0(2)	O(8)−S(3)−O(9)	118.6(2)
Sb(1)−O(1)−S(1)	137.2(2)	Sb(1)[e]−O(2)−S(1)	145.3(2)
Sb(1)[d]−O(3)−S(1)	151.4(2)	Sb(1)−O(4)−S(2)	145.8(2)
Sb(1)[e]−O(5)−S(2)	150.0(2)	Sb(1)[f]−O(6)−S(2)	149.9(2)
Sb(1)−O(7)−S(3)	138.8(2)	Sb(1)[b]−O(8)−S(3)	140.7(2)
Sb(1)[f]−O(9)−S(3)	159.6(2)		

[a] Symmetry operations: (a) $y, -x + y, 1/6 + z$; (b) $1 - x + y, 1 - x, 1/3 + z$; (c) $1 + x - y, x, -1/6 + z$; (d) $1 - y, x - y, -1/3 + z$; (e) $x - y, x, -1/6 + z$; (f) $y, 1 - x + y, 1/6 + z$.

The identification of the oxidation state of antimony as +3 rather than +1 as had been claimed[4] is supported by three observations:

(i) The colorless solutions are ESR silent and all solid precipitates from these solutions are diamagnetic, which argues against the presence of monomeric Sb(I) where a triplet ground state is expected.

(ii) Hydrolysis of the solid products in 4 M aqueous HCl gives colorless, clear solutions. Gas evolution or formation of elemental antimony is not observed. This behavior is not consistent with the presence of cyclic or polyhedral clusters of the composition $[Sb_n]^{n+}$ as suggested for $Sb[AsF_6]$.[6]

(iii) In these acidic, aqueous solutions the antimony content is reliably and reproducibly determined by the oxidation of Sb(III) with $KBrO_3$, using a standard procedure.[12,13] The analytical results for crystalline $[SbF_2(SO_3F)]_x$ and $[Sb(SO_3F)_3]_x$

are consistent with the composition established by X-ray diffraction.

The bromometric determination of the antimony(III) content[12,13] is in our view the most reliable method of analysis for the white solids. Sulfur determinations give very high values, while fluoride values are consistently low, probably on account of incomplete hydrolysis of the antimony fluoride species, and it is conceivable that the white material has been misanalyzed previously.[4] Sulfur is determined in our department as $BaSO_4$ in alcoholic solution after combustion of the sample and subsequent cation exchange to remove metallic elements but in this case not antimony. It is likely that barium antimonate is produced and interferes in the sulfate determination.

A final argument against the presence of $Sb(SO_3F)$ is provided by the crystal structures of the principal components of the mixture, which are reported here. It may be argued that heating the HSO_3F solution to 50 °C in order to effect separation from S_8 will result in more extensive self-dissociation of fluorosulfuric acid[19] according to

$$HSO_3F \rightleftharpoons HF + SO_3 \qquad (1)$$

and cause enhanced oxidizing ability of the medium, so that initially formed univalent antimony is oxidized further to Sb(III) during product separation. However, in the product mixture formed during the reaction of Sb with HSO_3F at 25 °C, only Sb(III) is present according to the three observations listed above. From the reaction, following product separation by hot filtration and recrystallization from HSO_3F, $[SbF_2(SO_3F)]_x$ is obtained (yield 61%) as described in the Experimental Section. The amount obtained in this manner is large enough for a structure determination, the recording of vibrational spectra, and microanalysis for Sb. The other fluoride fluorosulfate derivative $[SbF(SO_3F)_2]_x$ is obtained in very small amounts only, sufficient for a single-crystal structure determination and an IR spectrum. The method of preparation, the initial oxidation of Sb by bis(fluorosulfuryl) peroxide, followed by subsequent treatment with HSO_3F and separation from S_8 produces primarily $[Sb(SO_3F)_3]_x$. This conclusion is based on the vibrational spectra discussed below.

An alternate route to $[SbF_2(SO_3F)]_x$ is found in the solvolysis of $SbF_2(OC_2H_5)$[14] in HSO_3F. The starting material is prepared as reported previously[14] by a ligand redistribution reaction between SbF_3 and $Sb(OC_2H_5)_3$ in acetonitrile and isolated as a solid precipitate formed in this reaction. The other redistribution product, $SbF(OC_2H_5)_2$, is reportedly[14] soluble in CH_3CN and obtainable after removal of the solvent *in vacuo*. Our observations point to an equilibrium in CH_3CN solution, which suggests further ligand redistribution according to

$$2SbF(OC_2H_5)_2 \rightleftharpoons SbF_2(OC_2H_5) + Sb(OC_2H_5)_3 \qquad (2)$$

so that pure $SbF(OC_2H_5)_2$, which would be a suitable precursor for synthesis of $SbF(SO_3F)_2$, is not produced in this manner, even though satisfactory analytical data for S, C, and H are obtained. A possible alternate route to this compound, the reaction of $[Sb(SO_3F)_3]_x$ and $[SbF_3]_x$ in HSO_3F at a 2:1 mole ratio leads to a product mixture. It hence appears that even though the molecular structure of $[SbF(SO_3F)_2]_x$ is obtained (*vide infra*), we have been unable so far to produce sufficiently large quantities of this compound to permit microanalysis and the recording of good quality IR and Raman spectra.

Equally unsuccessful are attempts to obtain antimony(III) fluorosulfate, $[Sb(SO_3F)_3]_x$, by solvolysis reactions in HSO_3F according to

$$SbX_3 + 3HSO_3F \rightarrow [Sb(SO_3F)_3] + 3HX \qquad (3)$$

$$X = Cl \text{ or } OC_2H_5$$

In the case of X = Cl, the reaction is slow and incomplete. In the case of the solvolysis of $Sb(OC_2H_5)_3$ in HSO_3F, the main product is $[SbF_2(SO_3F)]_x$ according to the Raman spectrum. The use of HSO_3F as fluorinating agent has a fair number of precedents.[20] Its use as oxidizing agent toward a limited number of metals has been the subject of a preliminary study.[5]

The previously reported oxidation of antimony by bis(fluorosulfuryl) peroxide in HSO_3F[4] is used by us to prepare $[Sb(SO_3F)_3]_x$ according to

$$2Sb + 3S_2O_6F_2 \xrightarrow{HSO_3F} 2Sb(SO_3F)_3 \qquad (4)$$

A small excess of $S_2O_6F_2$ is employed to ensure complete and efficient oxidation. Any Sb(V) species so produced, *e.g.* $SbF_3(SO_3F)_2$ or $SbF_4(SO_3F)$,[7] remain in solution, and $[Sb(SO_3F)_3]_x$ is isolated as a white solid by filtration. Recrystallization from HSO_3F affords suitable single crystals for a molecular-structure determination.

It is interesting to note that in addition to $[Sb(SO_3F)_3]_x$, the two fluoride fluorosulfates of antimony(III), $[SbF_2(SO_3F)]_x$ and $[SbF(SO_3F)_2]_x$, are well-defined crystalline compounds with molecular, polymeric structures. In contrast, the corresponding antimony(V) fluoride fluorosulfates of the composition $SbF_n(SO_3F)_{5-n}$, n = 4.5 to 3, are viscous liquids[7,21] that are better viewed as nonstoichiometric phases,[21b] where the composition depends on the synthetic route chosen, the reactant ratio, and the subsequent treatment of the products (cooling, heating, or distillation) due to rapid F *vs* SO_3F exchange and the facile conversion of $-SO_3F$ to $-F$ and *vice versa* by SO_3-elimination or SO_3-insertion reactions. The low solubility of all three new materials in HSO_3F at ambient temperatures precludes meaningful ^{19}F NMR studies, which would shed some light on the formation of the polymeric species in solution.

In summary, our attempts to obtain $Sb(SO_3F)$ and characterize univalent antimony from the reaction of HSO_3F with Sb have not been successful. However, the possibility still exists that univalent antimony is present in $Sb[AsF_6]$ as claimed.[6] A more extensive characterization of this material is desirable.

Molecular Structures of Antimony(III) Difluoride Fluorosulfate $[SbF_2(SO_3F)]_x$, Antimony(III) Fluoride Bis(fluorosulfate) $[SbF(SO_3F)_2]_x$, and Antimony(III) Tris(fluorosulfate) $[Sb(SO_3F)_3]_x$. All three materials are polymers due to both fluoro- and fluorosulfato bridges. Hence formulation as $[SbF_2(SO_3F)]_x$, $[SbF(SO_3F)_2]_x$, and $[Sb(SO_3F)_3]_x$, respectively, appears more appropriate than the formulas based on the composition.

Stereoviews of the three structures are shown in Figures 1−3. The complete coordination environments of antimony in all three structures are shown in Figures 4−6. The primary coordination environment for $[Sb(SO_3F)_3]_x$ is shown in Figure 7.

The three structures belong to three different crystal systems, as seen in Table 1. Coordination numbers and geometries differ for all three. As a common feature, all three structure

(19) Thompson, R. C. In *Inorganic Sulphur Chemistry*; Nickless, G., Ed.; Elsevier: Amsterdam, The Netherlands, 1968; p 821.

(20) Engelbrecht, A. *Angew. Chem., Int. Ed. Engl.* **1965**, *4*, 641.

(21) (a) Gillespie, R. J.; Rothenbury, R. A. *Can. J. Chem.* **1964**, *42*, 416. (b) Willner, H.; Mistry, F.; Aubke, F. *J. Fluorine Chem.* **1992**, *59*, 333.

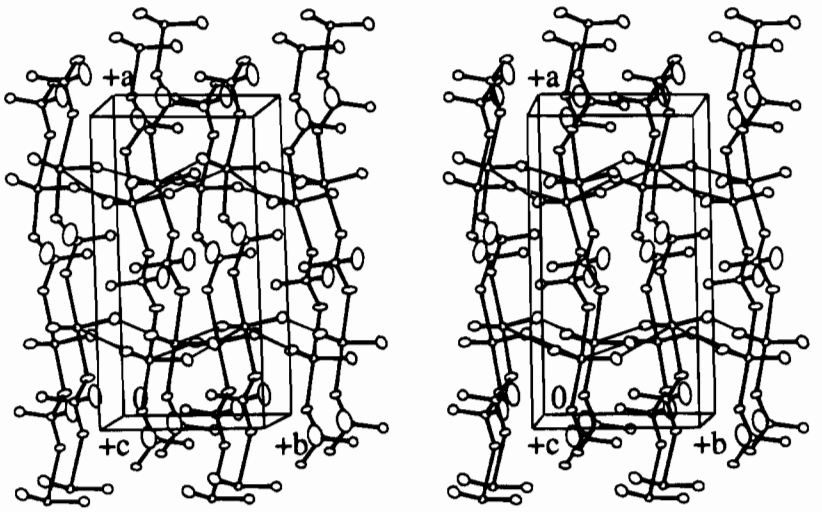

Figure 1. Stereoview of the structure of $[SbF_2(SO_3F)]_\infty$.

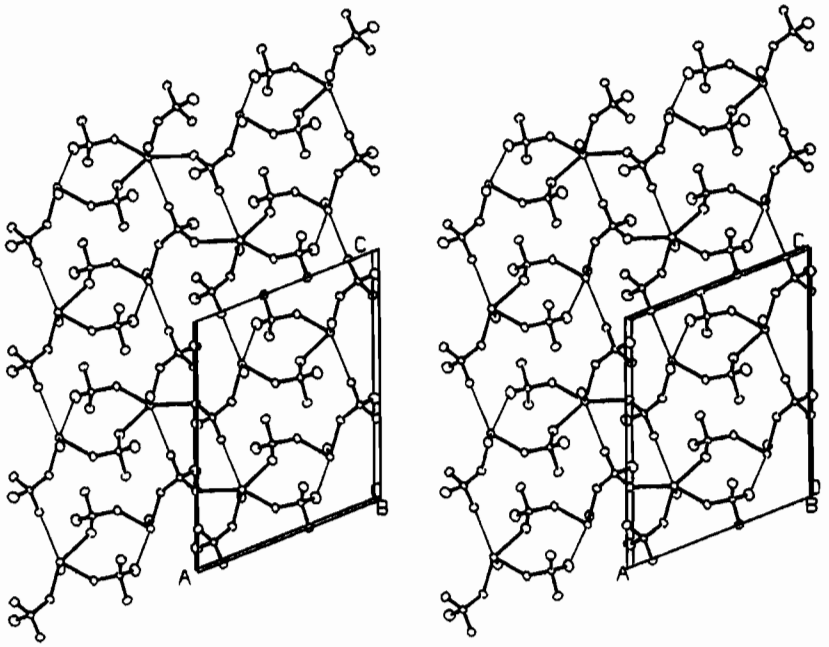

Figure 2. Stereoview of the structure of $[SbF(SO_3F)_2]_\infty$.

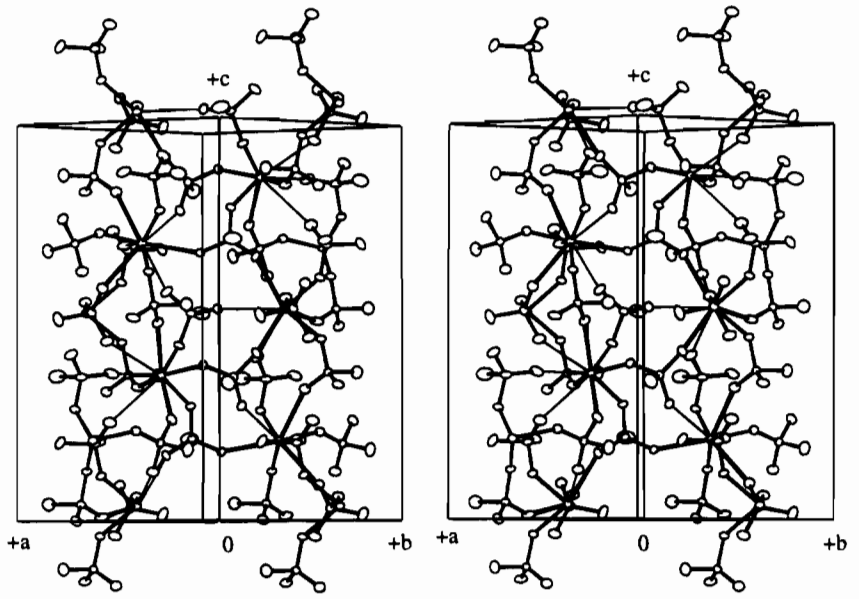

Figure 3. Stereoview of the structure of $[Sb(SO_3F)_3]_\infty$.

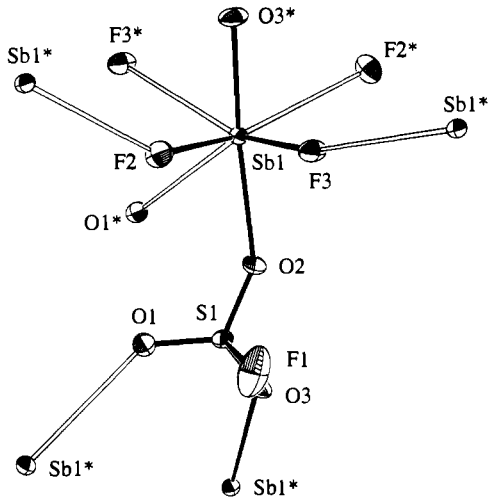

Figure 4. Perspective view of the complete antimony coordination environment in $[SbF_2(SO_3F)]_x$. 33% probability thermal ellipsoids are shown.

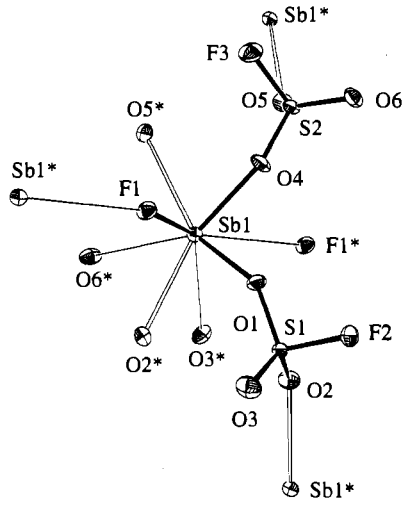

Figure 5. Perspective view of the complete antimony coordination environment in $[SbF(SO_3F)_2]_x$. 33% probability thermal ellipsoids are shown.

determinations are of very high accuracy and R_w values (for Mo $K\alpha$ data to $2\theta = 100°$) are 0.026 for $[SbF_2(SO_3F)]_x$ and 0.027 for the other two. As can be seen in Tables 3, 5, and 7, standard deviations are small, which permits an extensive discussion of bonding and stereochemistry for all three compounds. Even though the structure of $[SbF_3]_x$, the fourth member in the series $[SbF_n(SO_3F)_{3-n}]_x$, $n = 0$, 1, 2, or 3, was reported in 1970,[9] the structure determination is of sufficiently high quality that it can be included safely in a structural comparison.

Solid state structures of main group derivatives with the central atom below maximum valency are generally very complex, and bond distances around the central atom range from short, approximately covalent bond lengths to secondary contacts,[22] only slightly shorter than the sum of the van der Waals radii. The three molecular structures reported here are no exception to these general observations. For a number of antimony(III) halides and some related derivatives, this structural complexity is emphasized in a review[23] where the stereochemistry of antimony is discussed in terms of the VSEPR concept.[24]

In this study we start with focusing attention on the two ligands. As in $[SbF_3]_x$,[9] fluorine functions as a bidentate,

(22) Alcock, N. W. *Adv. Inorg. Chem. Radiochem.* **1972**, *15*, 1.
(23) Sawyer, J. F.; Gillespie, R. J. *Prog. Inorg. Chem.* **1986**, *34*, 65.

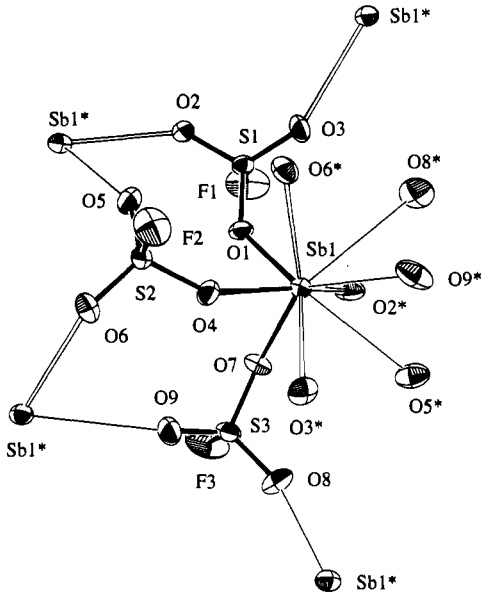

Figure 6. Perspective view of the complete antimony coordination environment in $[Sb(SO_3F)_3]_x$. 33% probability thermal ellipsoids are shown.

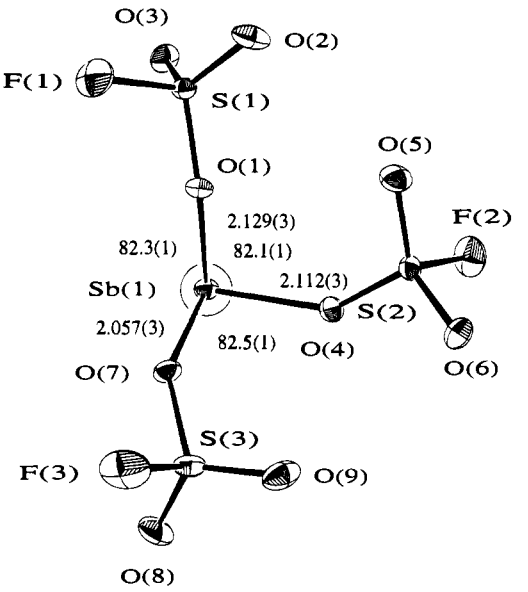

Figure 7. Perspective view of the primary antimony coordination environment in $[Sb(SO_3F)_3]_x$. 33% probability thermal ellipsoids are shown. Bond lengths are in Å, and angles are in degrees.

asymmetrical ligand in $[SbF_2(SO_3F)]_x$ and $[SbF(SO_3F)_2]_x$; however, both the short and the long Sb−F bond distances differ in all three structures. The fluorosulfate group is coordinated over all three O atoms, while the F−(S) atom is not involved in coordination or secondary contacts less than the sum of the van der Waals radii. Again all three Sb−O bond distances and all three S−O bond lengths for each fluorosulfate group differ. As a consequence of gradually replacing a bidentate ligand (F) by a tridentate one (SO_3F) in the series $[SbF_n(SO_3F)_{3-n}]_x$, the overall coordination number increases from 6 for $[SbF_3]_x$ to 7 for $[SbF_2(SO_3F]_x$, 8 for $[SbF(SO_3F)_2]_x$, and finally 9 for $[Sb(SO_3F)_3]_x$, as can be seen in Figures 4−6.

Because of the strongly asymmetric bridging of all ligands, the resulting coordination geometries are highly irregular and

(24) (a) Gillespie, R. J. *The VSEPR Model of Molecular Geometry*; Van Norstrand Reinhold: London, 1972. (b) Gillespie, R. J.; Hargittai, I. *The VSEPR Model of Molecular Geometry*; Allyn and Bacon: Boston, MA, 1991.

Table 8. Bond Distances and Angles for the Primary Coordination Geometries of the $[SbF_n(SO_3F)_{3-n}]$ (n = 3, 2, 1, or 0) Compounds

species and geometry	point group	bond dist (Å)[a]		bond angles (deg)[a]
$[SbF_3]$[b]		Sb-F(1)	Sb-F(2)	F(1)-Sb-F(1)
trigonal pyramid	C_{3v}	1.94(2)	1.90(2)	88.9 (1.5)
SbF(1)F(1)F(2)				
$[SbF_2(SO_3F)]_x$		Sb-F(2)	Sb-O(2)	F(2)-Sb-F(3) 88.4(2)
distorted square	~ C_{2v}	1.896(3)	2.342(3)	F(2)-Sb-O(3) 83.2(1)
pyramid		Sb-F(3)	Sb-O(3)	F(3)-Sb-O(2) 75.6(1)
SbF(2)O(2)F(3)O(3)		1.927(3)	2.204(3)	O(2)-Sb-O(3) 157.1(2)
$[SbF(SO_3F)_2]_x$		Sb-F(1)	Sb-O(4)	F(1)-Sb-O(1) 85.66(6)
trigonal pyramid	C_s	1.893(1)	2.131(1)	F(1)-Sb-O(4) 86.43(7)
SbO(1)O(4)F(1)			Sb-O(1)	
			2.113(1)	O(1)-Sb-O(4) 75.71(6)
$[Sb(SO_3F)_3]_x$		Sb-O(1)	Sb-O(4)	O(1)-Sb-O(4) 82.1(1)
trigonal pyramid	C_{3v}	2.129(3)	2.112(3)	O(1)-Sb-O(7) 82.3(1)
SbO(1)O(4)O(7)		Sb-O(7)		O(4)-Sb-O(7) 82.5(1)
		2.057(3)		

[a] The reference systems for atoms are adopted from ref 9 or from Figures 4, 5, or 6. [b] Reference 9.

descriptions are approximate. The distorted octahedron of $[SbF_3]_x$[9] changes to a pentagonal bipyramid for $[SbF_2(SO_3F)]_x$ (Figure 4) and a face-capped pentagonal bipyramid for $[SbF(SO_3F)_2]_x$ (Figure 5). In $[Sb(SO_3F)_3]_x$ we may view the coordination geometry as a tricapped highly irregular octahedron (Figure 6). The octahedron is formed by three primary short Sb−O bonds (~2.1 Å) arranged in the form of a trigonal pyramid and three secondary Sb−O contacts (~3.0 Å) as nearly linear extensions of the primary bonds, as is commonly observed for secondary bonds.[22] Capping involves the three remaining O atoms, which form a trigonal, approximately planar coordination environment for Sb with Sb−O ~ 2.6 Å. The three-dimensional polymer is of relatively high symmetry, and a 6-fold screw axis is discernible (see Figure 3). As rough guidelines for a further discussion, the sum of the covalent single-bond radii for Sb−O and Sb−F are 2.07 and 2.05 Å,[25] while the sum of the van der Waals radii are 3.57 and 3.52 Å for Sb−O and Sb−F, respectively.[26] These calculated distances are very approximate, because the radii for Sb usually pertain to pentavalent antimony.

Short Sb−F and Sb−O bonds and the angles between these bonds define the primary coordination geometries. The relevant data are collected in Table 8 for all four members in the series $[SbF_n(SO_3F)_{3-n}]$, n = 0−3. For $[SbF_3]_x$,[9] $[SbF(SO_3F)_2]_x$, and $[Sb(SO_3F)_3]_x$, the primary geometry is best described as a trigonal pyramid. Sb−F bond distances (~1.9 Å) are shorter and Sb−O distances (~2.1 Å) longer than the sums of the covalent radii. As can be seen from the interatomic distances in Tables 3, 5, and 7, even where O is strongly coordinated to antimony, the S−O bonds retain some multiple bond character, as will be discussed below. Consequently bond angles at antimony involving F are less acute than those involving O, but all are well below 90°. In VSEPR terms[24] all three primary coordination geometries are of the EAX_3 type. In our view the primary geometries are produced by repulsions between electrons in primary bonds and those in intermediate and secondary bonds, rather than by an imaginary lone electron pair of enormous space requirements, judging by the very acute bond angles observed.

A different primary geometry is observed for $[SbF_2(SO_3F)]_x$ on account of a slightly asymmetrical (Sb−O = 2.204(3) and 2.342(3) Å) bidentate bridging fluorosulfate group with slightly longer Sb−O bonds than in $[SbF(SO_3F)_2]_x$ and $[Sb(SO_3F)_3]_x$. Here a triangular SbF_2 moiety (bond angle 88.4(2)°) is expanded by an almost linear SbO_2 grouping (bond angle 157.1(2)°) into a very distorted square pyramid. In VSEPR terms[24] the structure may be described as $EAX_2X'_2$, derived from a trigonal bipyramid with F in equatorial and O in axial positions, but again the lone pair would have to be sterically very demanding to produce an SbF_2 angle of 88.4(2)°, about 31.6° more acute than a normal equatorial angle. Here, as discussed above, the geometry around antimony is in our opinion determined by electron density in primary, intermediate, and secondary bonds formed by antimony rather than by a stereochemically active lone pair.

In $[SbF_2(SO_3F)]_x$ intermediate bonding is exemplified by the asymmetric bridging fluorine ligands with bond lengths of 2.687(2) and 2.828(3) Å, respectively, slightly longer and more asymmetrical than in SbF_3[9] (2.60 and 2.63 Å). As seen in Figures 1 and 4, formation of fluoro bridges expands the primary coordination polyhedron into an irregular octahedron with O in trans positions and links polymeric $SbF_2(\mu\text{-}SO_3F)$ chains into corrugated, polymeric sheets. Further crosslinking of sheets is achieved by a secondary bond (2.946(3) Å) between Sb and the third oxygen of the fluorosulfate group.

The term "intermediate bonds" introduced in the preceding section refers to bonds lengths that are intermediate between covalent bonds and secondary contacts close to the sum of the van der Waals radii. This concept is best illustrated by the structures of $[SbF(SO_3F)_2]_x$ and $[Sb(SO_3F)_3]_x$, where the asymmetrically bridging fluorosulfate groups form intermediate, in addition to primary covalent and secondary, bonds. Primary covalent bonds are formed in both cases by one oxygen of each SO_3F group. The range of Sb−O distances, as seen in Table 8, is 2.057(3)−2.131(1) Å, comparable or slightly longer than the sum of the covalent radii.[25] A second oxygen atom of each fluorosulfate group forms an intermediate bond to antimony with Sb−O bond distances in a range 2.475(2)−2.566(1) Å in $[SbF(SO_3F)_2]_x$ to 2.550(3)-2.642(3) Å in $[Sb(SO_3F)_3]_x$. Here the intermediate bonds form an approximately trigonal planar coordination environment around antimony. Finally the third oxygen atom of each SO_3F group is involved in secondary bonding with Sb−O distances of 2.995(2) and 3.055(2) Å for $[SbF(SO_3F)_2]_x$ and of 2.834(3), 2.997(3), and 3.009(4) Å for $[Sb(SO_3F)_3]$.

In addition, in $[SbF(SO_3F)_2]_x$, secondary bonding involves also the F atom attached to Sb in bridging fashion. The Sb−F···Sb bridge is highly asymmetric (1.893(1) and 3.098(2) Å), more so than in SbF_3[9] or $[SbF_2(SO_3F)]_x$, and deviates substantially from linearity with Sb−F···Sb = 157.35(7)°.

With covalent[25] and secondary bonding[22] firmly established and documented in subvalent main-group compounds, the concept of intermediate bonding introduced serves to underscore the complexity of the three structures reported here. In this formally related group of the type $[SbF_n(SO_3F)_{3-n}]_x$, n = 0, 1, or 2, no two Sb−O or Sb−F bond distances or bond angles are the same, and different coordination geometries are encountered in all three cases. These geometries appear to be arrived at by using two or three available donor sites on F or SO_3F, respectively, in asymmetric bridging interactions, to form primary, intermediate, and secondary bonds to antimony, rather than by lone pair/bonding pair repulsions. The VSEPR model,[24] which had been inadequate to explain the observed bond angles

(25) Pauling, L. *The Nature of the Chemical Bond*, 2nd ed.; Cornell University Press: Ithaca, NY, 1948.
(26) Bondi, A. *J. Phys. Chem.* **1964**, *68*, 441.

Table 9. Internal S−O Bond Distances and the Corresponding O−Sb Interactions for $[SbF_2(SO_3F)]_x$, $[SbF(SO_3F)_2]_x$, and $[Sb(SO_3F)_3]_x$

species	S−O bond length (Å)[a]		length of O−Sb interaction (Å)[a]	
$[SbF_2(SO_3F)]_x$	S(1)−O(1)	1.408(3)	O(1)···Sb	2.946(3)
	S(1)−O(2)	1.435(3)	O(2)−Sb	2.342(3)
	S(1)−O(3)	1.453(3)	O(3)−Sb	2.204(3)
$[SbF(SO_3F)_2]_x$	S(1)−O(1)	1.480(1)	O(1)−Sb	2.113(1)
	S(1)−O(2)	1.437(2)	O(2)- -Sb	2.475(2)
	S(1)−O(3)	1.407(2)	O(3)···Sb	3.055(2)
	S(2)−O(4)	1.473(1)	O(4)−Sb	2.131(1)
	S(2)−O(5)	1.435(2)	O(5)- -Sb	2.566(1)
	S(2)−O(6)	1.414(2)	O(6)···Sb	2.995(2)
$[Sb(SO_3F)_3]_x$	S(1)−O(1)	1.477(3)	O(1)−Sb	2.129(3)
	S(1)−O(2)	1.419(3)	O(2)- -Sb	2.550(3)
	S(1)−O(3)	1.417(3)	O(3)- -Sb*	2.642(3)
	S(2)−O(4)	1.474(3)	O(4)−Sb(1)	2.112(3)
	S(2)−O(5)	1.412(3)	O(5)···Sb*	2.834(3)
	S(2)−O(6)	1.421(3)	O(6)- -Sb*	2.615(3)
	S(3)−O(7)	1.496(3)	O(7)−Sb	2.057(3)
	S(3)−O(8)	1.417(3)	O(8)···Sb*	3.009(3)
	S(3)−O(9)	1.407(3)	O(9)···Sb*	2.977(3)

[a] The numbering systems for atoms are adopted from Figures 4−6. The number for Sb is omitted.

for the primary coordination polyhedra, loses it great advantage, the enormous simplicity of the concept, in the face of the structural complexity encountered here. The Sb(III) halide structures reviewed some time ago[23] involve almost exclusively bidentate bridging ligands, which results in reduced structural complexity. The VSEPR model provides a useful guide in most cases discussed in this review.[23]

For the fluorosulfate groups in the three structures of the type $[SbF_n(SO_3F)_{3-n}]_x$ with $n = 0$, 1, or 2, an additional relationship is apparent. As the Sb−O distances vary between primary (~2.1 ± 0.1 Å), intermediate (~2.6 ± 0.1 Å), and secondary bonds (~3.0 ± 0.1 Å), so do, in an inverse manner, the S−O distances, over a considerably narrower range. This inverse relationship between S−O bond distances and O−Sb bonding interactions is apparent from the data summarized in Table 9. Only for $[Sb(SO_3F)_3]_x$, where steric crowding for the three fluorosulfate ligands may be anticipated, two departures from this relationship are noted affecting intermediate and secondary Sb−O contacts. The observed narrow range of S−O bond distances of 1.407(3)−1.496(3) Å extends to both sides of d(S−O) in ionic SO_3F^- [27] (1.43 Å). As expected, variations in S−F distances are very small and are within error limits ~ 1.539 Å. Fluorine attached to sulfur is not involved in coordination to antimony, which is also apparent from its relatively large thermal ellipsoids in Figures 4−6. Only for $[SbF_2(SO_3F)]_x$ is a very slightly shorter S−F bond distance (1.529(3) Å) noted; however, here the primary coordination sphere and the coordination mode of the SO_3F group are different as discussed above.

In addition to the secondary contacts between Sb and O or F, there are numerous additional, nonbonded interactions in each of the polymeric structures. Interactions of this type with interatomic distances between 3.00 and 3.60 Å are included in the supplementary material for the three structures reported here.

Comparison to Related Structures. Very few solid fluoride fluorosulfates of low-valent main-group elements are known. Of these, only $FXe(SO_3F)$[28] is structurally characterized. The molecular structure is rather straightforward. The coordination environment of xenon is linear, the SO_3F group is monodentate, and the S−O bond distances for the noncoordinated O-atoms are identical within error limits.

More relevant to our discussion is the reported molecular structure of $Sn(SO_3F)_2$,[29a] which is recent and highly accurate. As in $[SbF_2(SO_3F)]_x$, the primary coordination geometry is described in VSEPR terms as AX_4E, and inclusion of two longer Sn-O contacts also results in a distorted octahedral environment, similar to the one shown here in Figure 5. There is also comparable complexity, and as in $[SbF(SO_3F)_2]_x$, the two SO_3F groups are structurally different.

The short primary Sn-O bond distances are somewhat longer than Sb−O bonds in $[SbF_2(SO_3F)]_x$ and fall between 2.338(3) and 2.427(3) Å. Consequently the range of the corresponding S−O distances is narrower (1.404−1.457 Å) and it appears also that F, bonded to sulfur, may be involved in a long-range interaction with tin. The narrow range of Sn−O primary bonds makes it more appropriate to use in the VSEPR concept.[24] For $[SbF_2(SO_3F)]_x$ this range is between 1.896(3) (Sb−F) and 2.342(3) Å (Sb−O) and consequently all polyhedra are hugely distorted.

Differences in element−oxygen primary bond distances between $Sn(SO_3F)_2$[29a] and $[SbF_2(SO_3F)]_x$ may in part be due to differences in the radii for Sn(II) and Sb(III), respectively, and in part to slightly reduced steric crowding in the primary coordination sphere for $[SbF_2(SO_3F)]_x$, where only two rather than four fluorosulfate groups are involved in coordination to the central atom.

As discussed above, a good structural comparison is possible between $[SbF(SO_3F)_2]_x$ and $[SbF_3]_x$,[9] even though the structure of the latter compound was published in 1970 and is less accurate (larger esd's), but this comparison is restricted to the primary coordination sphere because F^- functions as an asymmetric bidentate bridge, restricting the maximum coordination number to 6. On the other hand, $[SbF_3]_x$ is a classical example of secondary bonding,[22] where secondary contacts are nearly linear extensions of the shorter primary bonds in the opposite direction.

The review on Sb(III) halides by Sawyer and Gillespie[23] contains many more pertinent examples of complex geometries similar to those encountered here. We have not included these examples because many of the examples discussed are anions with slightly longer Sb−F bonds and molecular polydentate bridging ligands like the SO_3F group are only rarely encountered among them.[23]

A formal similarity exists between $[Sb(SO_3F)_3]_x$ and $[Au(SO_3F)_3]_2$,[29b] the only other metal tris(fluorosulfate) where the molecular structure is known. However, as the formula indicates, gold tris(fluorosulfate) is dimeric, the coordination environment is approximately square planar, commensurate with a d^8 electron configuration, and mono- and bidentate fluorosulfate groups are encountered. Only a few weak and long intermolecular contacts between gold and oxygen are noted that contribute to an elongated, strongly distorted octahedral coordination environment for gold. All these features are in strong contrast to observations made here for $[Sb(SO_3F)_3]_x$.

Finally a number of sulfato derivatives of Sb(III) have been structurally characterized in the 1970s. They are formulated as $Sb_2O_3 \cdot 2SO_3$,[30] $Sb_2SO_3 \cdot 3SO_3$,[31] and $Sb_2(S_2O_7)_3$.[32] We have

(27) O'Sullivan, K.; Thompson, R. C.; Trotter, J. *J. Chem. Soc. A* **1967**, 2024.
(28) Bartlett, N.; Wechsberg, M.; Jones, G. R.; Burbank, R. D. *Inorg. Chem.* **1972**, *11*, 1124.
(29) (a) Adams, D. C.; Birchall, T.; Faggiani, R.; Gillespie, R. J.; Vekris, J. E. *Can. J. Chem.* **1991**, *69*, 2122. (b) Willner, H.; Rettig, S. J.; Trotter, J.; Aubke, F. *Can. J. Chem.* **1991**, *61*, 391.
(30) Mercier, R.; Douglade, J.; Theobald, F. *Acta Crystallogr.* **1975**, *B31*, 2081.
(31) Mercier, R.; Douglade, J.; Bernard, J. *Acta Crystallogr.* **1976**, *B32*, 2787.
(32) Douglade, J.; Mercier, R. *Acta Crystallogr.* **1979**, *B35*, 1062.

not included them in our discussion because emphasis is placed on the primary coordination spheres of sulfur and antimony, where rather similar Sb−O distances to the ones observed by us are found.[30−32] Secondary or intermediate interactions are frequently not included in the discussion, and the bonding interpretation appears to be uneven and occasionally lacking in sophistication. The structure of $Sb_2O_3{\cdot}2SO_3$ is said to consist of pairs of SO_4 tetrahedra and SbO_3 trigonal pyramids sharing corners to form "blocks that are then linked by van der Waals bonds between oxygen atoms".[30] For $Sb_2O_3{\cdot}3SO_3$[31] intermediate and long-range Sb−O contacts of ~2.7−2.87 Å are noted and primary Sb−O bond distances as short as 2.028 Å are observed. It appears that the structural complexity encountered by us in the fluoride fluorosulfates of antimony(III) extends also to the sulfate derivatives,[30−32] but this may not have been recognized previously.

Vibrational Spectra. We have previously reported on a number of fluoride fluorosulfates, formed by main-group elements with the central atom in its maximum oxidation state. They include the solid polymeric materials $GeF_2(SO_3F)_2$,[33] $SnF_2(SO_3F)_2$,[34] and the liquid, oligomeric antimony(V) derivatives $Sb_2F_9(SO_3F)$,[7] $SbF_4(SO_3F)$,[7,20] and $SbF_3(SO_3F)_2$.[7] In all compounds, octahedral coordination of the central atom, the presence of symmetrically bridging fluorosulfate groups, and terminal fluoro ligands had been suggested. Evidence has come mainly from vibrational spectra and, in the case of $SnF_2(SO_3F)_2$, from ^{119}Sn Mössbauer spectra.[34] In a number of molecular structures, *e.g.* those of $(CH_3)_2Sn(SO_3F)_2$,[35] $[Au(SO_3F)_3]_2$,[29b] and more recently $[Pd_2(\mu\text{-}CO)_2](SO_3F)_2$,[36] the presence of symmetrically bridging SO_3F groups has lent additional support for the structural conclusions regarding main-group element fluoride fluorosulfates.

It is of interest to record vibrational spectra of both $[SbF_2(SO_3F)]_x$ and $[SbF(SO_3F)_2]_x$ as well as of $[Sb(SO_3F)_3]_x$ to note the effect of decidedly asymmetrically bridging fluorosulfate groups in the two fluoride fluorosulfates on the vibrational bands, in particular the SO_3F-stretching region (1450−800 cm^{-1}). With the symmetry of the fluorosulfates in the two molecules reduced below C_{3v}, nine fundamentals, including four stretching modes for each SO_3F group, are expected. In addition, a comparison of the vibrational spectra for the two pairs $[SbF_2(SO_3F)]_x$ and $SbF_4(SO_3F)$[7] or $[SbF(SO_3F)_2]_x$ and $SbF_3(SO_3F)_2$ is of interest. The emphasis here is again on the SO_3F stretching vibrations and on the identification and assignment of the Sb−F vibrations, where asymmetric fluoro bridges are found for the two Sb(III) compounds.

In the case of $[SbF_2(SO_3F)]_x$, the crystalline material used in the X-ray study gives a well-resolved FT-IR spectrum. An identical spectrum is obtained from a sample formed by solvolysis of $SbF_2(OC_2H_5)$ in HSO_3F. The solvolysis of $Sb(OC_2H_5)_3$ in HSO_3F also produces surprisingly $[SbF_2(SO_3F)]_x$, and a Raman spectrum of the product is obtained. The vibrational bands for $[SbF_2(SO_3F)]_x$ are listed in Table 10 together with estimated band intensities.

The IR spectrum of $[SbF_2(SO_3F)]_x$ is simple. The Raman spectrum is of poorer quality and possibly incomplete. The band distribution in the SO_3F stretching region is very similar to that observed for $[Pd_2(\mu\text{-}CO)_2](SO_3F)_2$[36] ($\bar{\nu}(SO_3)$ at 1311, 1202, and 1083 cm-^{1}, $\bar{\nu}$(SF) at 823 cm^{-1} in the IR spectrum) and for $(CH_3)_2Sn(SO_3F)_2$[35] ($\bar{\nu}(SO_3)$ at 1351, 1189, and 1072 cm^{-1}, $\bar{\nu}$(SF) 827 cm^{-1}), where fluorosulfate anions are arranged in a bidentate bridging fashion, according to the molecular structures.[35,36] In $SbF_4(SO_3F)$ the SO_3F band distribution (Raman, $\bar{\nu}(SO_3)$ 1424, 1150, and 1080 cm^{-1}, $\bar{\nu}$(SF) 900 cm^{-1}) suggests a covalent bidentate SO_3F group. For O-bidentate SO_3F groups, the two SO_3 stretches at the highest wavenumbers may be taken to arise from the splitting of the asymmetric SO_3 stretch (E) for ionic SO_3F^-, usually at 1280 cm^{-1},[37] while the symmetric stretch (A_1) remains at about 1070−1080 cm^{-1}. The extent of E-mode splitting may be seen as an approximate measure of covalency. The splitting values for the four compounds discussed above are, in order of increasing wavenumbers, as follows: $[Pd_2(\mu\text{-}CO)_2](SO_3F)_2$, 109 cm^{-1}; $[SbF_2(SO_3F)]_x$, 143 cm^{-1}; $(CH_3)_2Sn(SO_3F)_2$, 162 cm^{-1}; $SbF_4(SO_3F)$, 274 cm^{-1}. Also $\bar{\nu}$(SF) bands will move to higher wavenumbers with increasing covalency and a similar trend is suggested.

Table 10. Vibrational Spectral Data for $[SbF_2(SO_3F)]_x$[a]

IR $\bar{\nu}$ (cm^{-1}), int	Raman $\Delta\bar{\nu}$ (cm^{-1}), int	approx description
1360 s, sh		
1348 vs	1350 ms	$\nu(SO)_3^{(b)}$
1246 ms, sh		
1204 vs	~1200 vw	$\nu(SO)_3^{(b)}$
	1161 m	
~1060 vs	1064 s	$\nu(SO)_3^{(b)}$
~1055 ms, sh		
819 vs	817 s	ν(SF)
612 s	617 m	$\delta(SO)_3^{(b)}$
~580 w, sh	587 m, sh	$\delta(SO)_3^{(b)}$
~565 m, sh	562 vs	$\nu(Sb{-}F_2)_{sym}$
554 vs	~550 w, sh	$\delta(SO_3)^{(b)}$
518 s	515 m, sh	
~512 m, sh	507 ms	$\nu(Sb{-}F)_{as}$
416 s	422 m	$\varrho(SO_3F)$
278 ms		
272 m, sh		$\varrho(SO)_3$

[a] Abbreviations: s = strong, m = medium, w = weak, v = very; sh = shoulder. (b) = bidentate bridging, sym = symmetric, as = asymmetric.

All three SO_3 stretches of $[SbF_2(SO_3F)]_x$ show more or less well-resolved shoulders in the IR spectrum, which may be caused by factor-group effects or by the unsymmetrical bridging configuration of the SO_3F group, as evidenced by the molecular structure. The proposed assignment of bands to Sb−F stretching modes is based on the observation of an unusually intense Raman band at 562 cm^{-1} with an IR counterpart at ~565 cm^{-1}, attributed to a symmetric Sb−F stretching vibration. The asymmetric stretch is attributed to bands at ~512 (IR) and 507 cm^{-1} (Raman), a region free of SO_3F bands both in $(CH_3)_2Sn(SO_3F)_2$[35] and $[Pd_2(\mu\text{-}CO)_2](SO_3F)_2$.[36] The occurrence of a symmetric stretch at higher wavenumbers than the corresponding asymmetric stretch is not uncommon for trihalides with pyramidal structures.[38]

The FT-IR spectrum of $[SbF_3]_x$ is of limited use. In addition to a weak band at 706 cm^{-1} and a strong shoulder at 607 cm^{-1}, there is an intense, very broad band centered at ~510 cm^{-1}. Not surprisingly for the Sb(V) fluoride fluorosulfates including $SbF_4(SO_3F)$,[7] the Sb−F stretching vibrations fall into the region of 640−730 cm^{-1} and are more readily distinguishable from the internal vibrational bands due to the fluorosulfate group. Here association *via* fluorosulfate bridges rather than fluoride bridging has been suggested.[7]

The infrared spectrum of $[Sb(SO_3F)_3]_x$, shown in Figure 8, is considerably more complex. Band positions and relative

(33) Mallela, S. P.; Lee, K. C.; Aubke, F. *Inorg. Chem.* **1984**, *23*, 653.
(34) Levchuk, L. E.; Sams, J. R.; Aubke, F. *Inorg. Chem.* **1972**, *11*, 43.
(35) Allen, F. A.; Lerbscher, J.; Trotter, J. *J. Chem. Soc. A* **1971**, 2507.
(36) Wang, C.; Bodenbinder, M.; Willner, H.; Rettig, S. J.; Trotter, J.; Aubke, F. *Inorg. Chem.* **1994**, *33*, 779.
(37) Ruoff, A.; Milne, J. B.; Kaufmann, G.; Leroy, M. *Z. Anorg. Allg. Chem.* **1970**, *372*, 119.
(38) Nakamoto, K. *Infrared Spectra of Inorganic and Coordination Compounds*; John Wiley and Sons: New York, 2nd ed.; 1970; p 93.

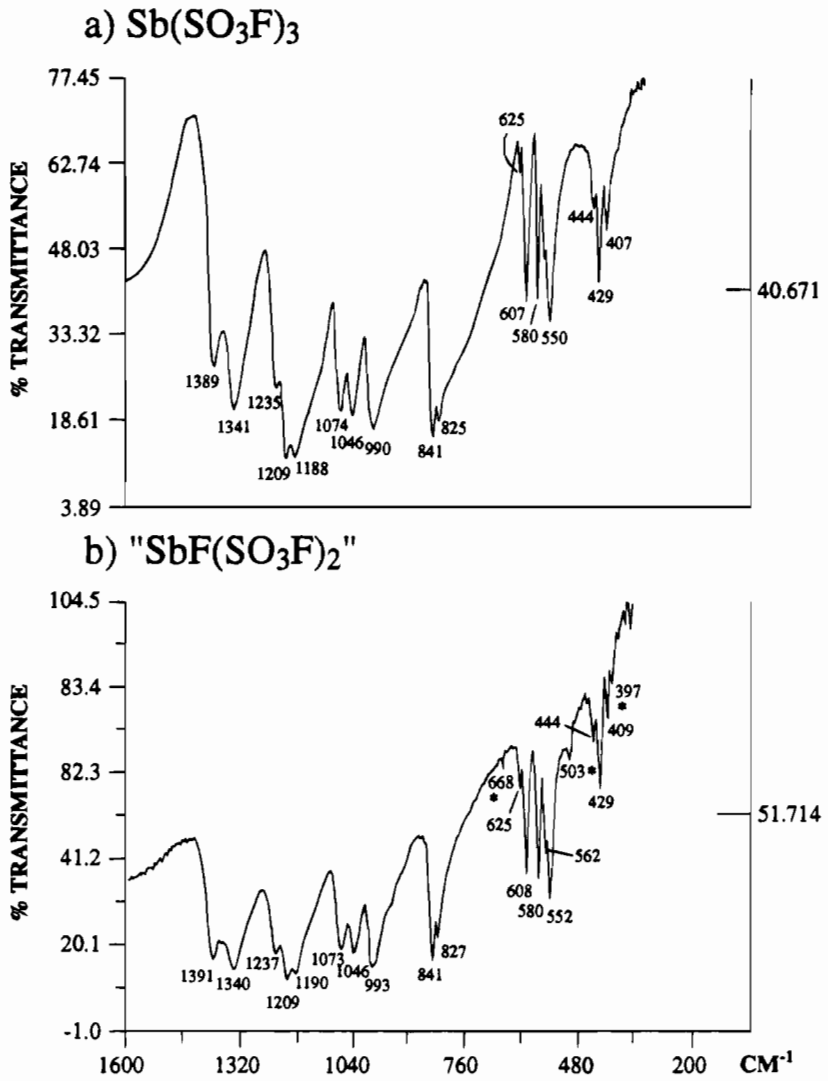

Figure 8. FT-IR spectra of $Sb(SO_3F)_3$ and "$Sb(SO_3F)_3$".

intensities for the IR and Raman spectra of this compound are listed in the Experimental Section. The complexity of the IR spectrum is not unexpected because the three fluorosulfate groups are nonequivalent. The observation of eight bands, attributable to SO_3-stretching vibrations, and of two $\bar{\nu}$(SF) bands at 841 and 827 cm^{-1} is consistent with the complex molecular structure. While vibrational coupling may be a contributing factor, the observed band proliferation does not allow a vibrational analysis in terms of the denticity of the SO_3F groups and the coordination geometry of antimony. This had been possible for other binary fluorosulfates, *e.g.* $[Au(SO_3F)_3]_2$,[39] with confirmation subsequently *via* the molecular structure determination,[29b] or for $Sn(SO_3F)_4$,[40] with support from ^{119}Sn Mössbauer spectroscopy, and for $Pt(SO_3F)_4$[41] or more recently for $Zr(SO_3F)_4$ and $Hf(SO_3F)_4$,[42] which all give rise to much simpler vibrational spectra. Hence only limited conclusions can be drawn from the spectrum. Band positions in the SO_3 stretching region extend from 1390 to 990 cm^{-1}, a considerably wider range than for $[SbF_2(SO_3F)]_x$ (see Table 10), suggesting stronger covalent interactions between Sb and the fluorosulfate. Bands in the 520-cm^{-1} region, attributed to Sb−F stretching (*vide supra*), are now absent. The fragmentary Raman spectrum has its most intense band at 871 cm^{-1}, assigned to an S-F stretch. We have previously noted equally intense Raman bands in this region for polymeric binary fluorosulfates of the type $M(SO_3F)_2$, M = Hg, Cd, or Zn,[43] which have, like many sulfonates of divalent metals,[44,45] a $CdCl_2$ layer structure, and conclude that polydentate bridging fluorosulfate ligands are present in antimony(III) fluorosulfate. The polymeric structure suggested by the vibrational data is consistent with the molecular structures reported here.

A surprising observation is made when the IR spectra for $[Sb(SO_3F)_3]_x$ and $[SbF(SO_3F)_2]_x$ are compared (see Figure 8). Except for weak bands at 668, 503, and 397 cm^{-1} and a slightly different shape of the band at 825 cm^{-1}, observed for the latter compound, both spectra are completely identical as judged by band position, relative band intensities, and band shapes. Unfortunately the amount of crystalline $[SbF(SO_3F)_2]_x$ had been small, and we were only able to obtain a rather poor IR spectrum, but no microanalysis, which in view of the completed structure determination for this material was considered initially unnecessary. It must be concluded that the bulk material obtained in the manner described in the Experimental Section is largely $[Sb(SO_3F)_3]_x$. This example shows that mistakes can easily be made where the composition of a material is inferred

(39) Lee, K. C.; Aubke, F. *Inorg. Chem.* **1979**, *18*, 389.
(40) Yeats, P. A.; Poh, B. L.; Ford, B. F. E.; Sams, J. R.; Aubke, F. *J. Chem. Soc. A* **1970**, 2188.
(41) Lee, K. C.; Aubke, F. *Inorg. Chem.* **1984**, *23*, 2124.
(42) Mistry, F.; Aubke, F. *J. Fluorine Chem.* **1994**, *68*, 239.
(43) Mallela, S. P.; Aubke, F. *Can. J. Chem.* **1984**, *62*, 382.
(44) Alleyne, C. S.; O'Sullivan-Mailer, K.; Thompson, R. C. *Can. J. Chem.* **1974**, *52*, 336.
(45) Lee, K. C.; Aubke, F. *Can. J. Chem.* **1977**, *55*, 2473.

solely from a completed crystal structure with single crystals obtained from the bulk material. Such mistakes are avoided by the use of microanalysis and vibrational spectroscopy. The data from an FT-IR spectrum of a genuine sample of $[SbF(SO_3F)_2]_x$ are given in the Experimental Section and depart from those of $[SbF_2(SO_3F)]_x$ or $[Sb(SO_3F)_3]_x$ as expected. The spectral complexity precludes a meaningful interpretation.

Summary and Conclusions

The initial objectives of this study, to confirm the existence of antimony(I) fluorosulfate, $Sb(SO_3F)$, and to provide a more detailed characterization of this material, have not been achieved. There is now considerable doubt as to whether antimony in the oxidation state +1 exists in thermodynamically stable, isolable compounds. An extensive study of the reaction between antimony and fluorosulfuric acid and the subsequent development of specific synthetic routes produces single crystals of the polymeric antimony(III) fluoride fluorosulfates $[SbF_2(SO_3F)]_x$, $[SbF(SO_3F)_2]_x$, and $[Sb(SO_3F)_3]_x$. The molecular structure determinations for all three compounds are of high accuracy and allow, together with the previously reported structure of $[SbF_3]_x$,[9] a detailed comparison for the series $[SbF_n(SO_3F)_{3-n}]_x$, with $n = 0$, 1, 2, or 3, and an insight into the complex coordination chemistry of Sb(III) toward hard, polydentate ligands like F^- and SO_3F^-. Both anions function here as bidentate (F) or O-tridentate (SO_3F) asymmetrically bridging ligands. The coordination number of antimony depends strictly on the available donor sites of the ligands and accordingly increases gradually from 6 for SbF_3 to 9 for $[Sb(SO_3F)_3]_x$. The coordination geometries are highly distorted and irregular and defy, in our opinion, descriptions using the VSEPR model.[24] In the solid state the primary interactions for $[Sb(SO_3F)_3]_x$ produce a trigonal pyramidal structure, illustrated in Figure 7, with very acute bond angles. Secondary interactions[22] (d(Sb- -O) ~ 3.0 Å) extend the coordination environment to a distorted trigonal antiprism, and intermediate bonds (d(Sb- -O) ~ 2.55−2.64 Å) arranged in a trigonal planar coordination complete the nine-coordinate structure. Sb−O and Sb−F interactions in all four compounds span the whole range from normal covalent bonds (1.9−2.1 Å) to ~ 3.0 Å and present a complicated bonding situation, which is not adequately accounted for by invoking the classical concepts of primary[25] and secondary[22] covalent bonding. Hence the concept of intermediate bonds, midway between covalent bonds and van der Waals contacts, is introduced. The relative weakness of intermediate bonds and secondary contacts is reflected in the fact that all three materials will dissolve on mild heating in HSO_3F and can be recrystallized easily from this medium. In addition $[Sb(SO_3F)_3]_x$, which is an intermediate in the oxidation of antimony by $S_2O_6F_2$, should be oxidizable further. Attempts by us have resulted very recently[46] in the isolation and structural characterization of $Cs[Sb(SO_3F)_6]$.

Acknowledgment. Financial support by the Natural Sciences and Engineering Research Council of Canada (NSERC) is gratefully acknowledged. We thank Carolyn Joyce for typing this manuscript.

Supplementary Material Available: Complete tables of crystallographic data, anisotropic thermal parameters, torsion angles, and nonbonded contacts (14 pages). Ordering information is given on any current masthead page.

IC941410P

(46) Zhang, D. L.; Rettig, S. J.; Trotter, J.; Aubke, F. *Inorg. Chem.* **1995**, *34*, 2269.